Corroded Tension Chord Model (CTCM) for concrete structures with locally corroded reinforcement

Author(s):
Häfliger, Severin; Yilmaz, Deniz; Angst, Ueli; Kaufmann, Walter

Publication date:
2020-12-01

Permanent link:
https://doi.org/10.3929/ethz-b-000458172

Corroded Tension Chord Model (CTCM) for concrete structures with locally corroded reinforcement

Severin Haefliger, Deniz Yilmaz, Ueli Angst and Walter Kaufmann

Institute of Structural Engineering, Institute for Building Materials,
ETH Zurich, Stefano-Franscini-Platz 3/5, 8093 Zurich, Switzerland

Abstract

Many ageing RC structures suffer from severe localised corrosion of the reinforcing bars, particularly if exposed to chlorides. This damage affects strength and ductility: The cross-section loss of the reinforcing bars reduces the load carrying capacity, and the highly localised damage results in a localisation of deformations, which may severely impair the structure's deformation capacity. A recent study at ETH Zurich investigated these effects on a sound mechanical basis, extending the established Tension Chord Model by corroded crack elements. This paper introduces the modelling concept of the resulting Corroded Tension Chord Model (CTCM) and presents the results of its application to structural elements with several corrosion spots. It reveals a significant decrease of the deformation capacity. Finally, an outlook on ongoing validation experiments is given.

1 Introduction

Many ageing reinforced concrete structures are affected by severe local and/or uniform corrosion due to e.g. chloride ingress or carbonation. Both deterioration processes lead to a considerable reduction of the load-bearing capacity, as they reduce the cross sectional area of the affected reinforcing bars. Additionally, localised corrosion leads to a strong reduction of the structure's deformation capacity, as beyond of a certain degree of damage, plastic strains only occur within the damaged section of the affected reinforcing bar: The damaged section undergoes yielding and hardening, whereas the undamaged sections of the same reinforcing bar remain elastic. Combined with the very small length of the damaged section, the integrated strains over length representing the deformation are reduced heavily compared to those of an undamaged reinforcing bar.

The reduced deformation capacity of concrete structures with locally corroded reinforcing bars is a major problem for structures, which are statically indeterminate, e.g. bridge decks of multispan bridges, or whose main loading is deformation dependent, e.g. the earth pressure action on cantilever retaining walls. While the outlined problem is recognised by the research community for bare reinforcing bars [1,2,3], to the authors knowledge, a sound mechanical model for the load-deformation behaviour at structural level is missing. This issue rises considerable uncertainty regarding the in any case very demanding assessment of existing structures.

To overcome this knowledge gap, in a recent study at ETH Zurich, the established Tension Chord Model (TCM) [4] was extended with a section containing a reinforcing bar with reduced cross section simulating corrosion induced damage. The resulting Corroded Tension Chord Model (CTCM) enables the calculation of the load-deformation behaviour of single tension chords and, by applying common mechanical concepts, also the behaviour of entire structural elements. It aims at providing a mechanically sound theoretical model for the relevant phenomena occurring in locally corroded structural elements, such as a strong decrease in deformation capacity, which has been observed in many experiments, e.g. [5,6]. This paper introduces the basic concept of the CTCM and analyses the effect of a localised corrosion on the load-bearing and deformation capacity of single tension chords and structural elements. Together with the conclusions, an outlook is given to an ongoing experimental campaign at ETH Zurich, aiming at validating the CTCM with experimental data.

2 TCM and CTCM Model description

2.1 Existing Tension Chord Model TCM

The established Tension Chord Model [4] was developed in the 1990s at ETH Zurich and describes the tension stiffening effect, i.e. the effect of bond on structural elements loaded in tension. It is a mechan-

ically consistent model, whose only empirical approximation consists in modelling the bond behaviour. The bond shear stress-slip behaviour $\tau_b - \delta$ is assumed to be rigid – ideally plastic with a value $\tau_b(\delta) = \tau_{b0} = 2f_{ct}$ for regions where the reinforcing bar remains elastic and $\tau_b(\delta) = \tau_{b1} = f_{ct}$ for regions where the reinforcing bar yields. This assumption enables to decouple the kinematic relations from the equilibrium of forces, and therefore to solve the differential equation of bond in closed form. Steel stresses of the reinforcing bar along a crack element, i.e. the tension chord element bounded by two cracks, are defined by the steel stress at the crack $\sigma_{s,r} = F/A_s$ and its continuous reduction induced by bond stresses (Fig. 1), i.e. $\sigma_s(x) = \sigma_{s,r} - 4x\varnothing\pi\tau_b/\varnothing^2\pi = \sigma_{s,r} - 4x\tau_b/\varnothing$, where Ø denotes the diameter of the reinforcing bar. Steel strains follow by transforming steel stresses using an appropriate constitutive relationship $\varepsilon_s = f(\sigma_s)$ (Fig. 1 and Tab. 1). Integrating the steel strains over the length of the crack element yields the deformation of the reinforcing bar $u_s = \int \varepsilon_s dx$ (Fig. 1). Crack widths can be determined by subtracting the deformation of the surrounding concrete $w_{cr} = u_s - u_c \approx u_s$. Practically, the concrete deformations are often ignored, as they are magnitudes smaller than the steel deformations.

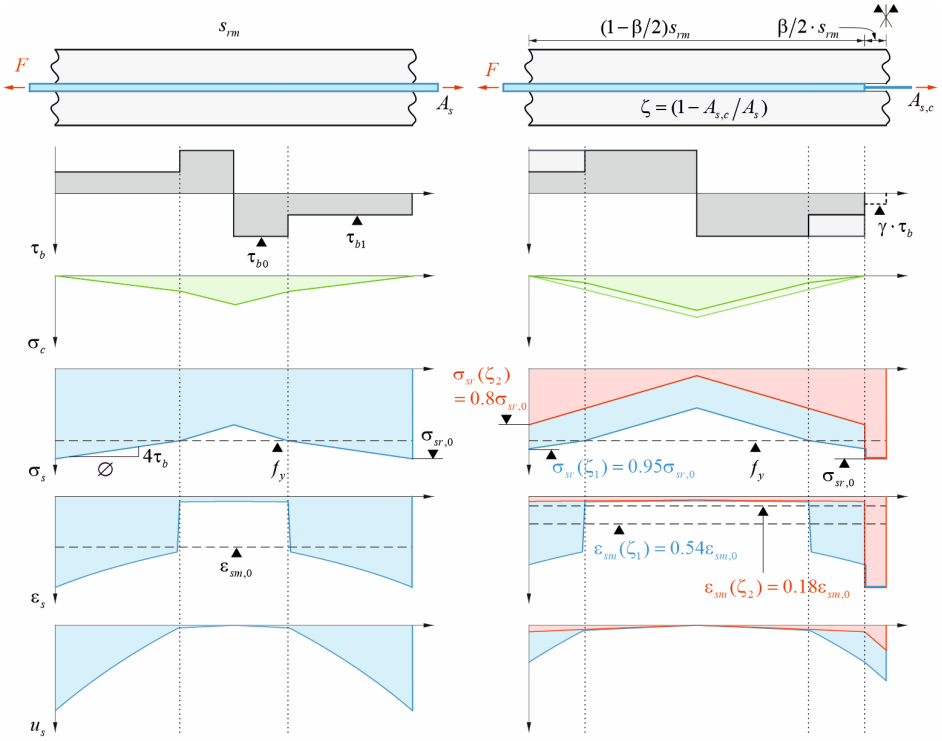

Fig. 1: TCM (left) and CTCM (right) with crack element of length s_{rm} and distributions of bond stress τ_b, stress in concrete σ_c, steel stress σ_s, steel strain ε_s, and steel deformations u_s. ε_{sm} denotes the mean steel strain over the entire crack element. For the CTCM (right), $\beta/2 \cdot s_{rm}$ denotes half of the length of the corroded section of the reinforcing bar. In blue, the results are given for a degree of corrosion $\zeta_1 = 0.05$, in red for $\zeta_2 = 0.17$.

Evaluating the TCM for small tensile loads allows analysing the cracking behaviour of a tension chord, i.e. the cracking load $\sigma_{sr,cr}$ and the crack spacing s_r, which is equivalent to the crack element length. Both values depend on the reinforcement ratio $\rho = A_s/A$, where A_s and A denote the areas of the reinforcing bar and of the whole tension chord section, respectively. Whereas the cracking load is a specific value, theoretical considerations show that the crack spacing can vary within the boundaries $s_{r1} = 0.5 \cdot s_{r0} \le s_r \le s_{r0}$, even in the theoretical case of a constant tensile strength without any scatter, since at the middle between two cracks with maximum spacing s_{r0}, a new crack may form or not [4]. The aspect, that it is not possible to predict the exact crack spacing by theoretical means, is very well represented by the highly variable crack spacings observed in laboratory tests on tension chords. Therefore, a mean crack spacing $s_{rm} = \lambda \cdot s_{r0}$ is introduced in the TCM ($0.5 \le \lambda \le 1$).

Despite the simplifications made on bond behaviour, the model reveals excellent agreement with experimental data. Because of its accuracy and its simplicity, it is widely applicable and builds part of many complex models such as the Cracked Membrane Model [7].

2.2 Corroded Tension Chord Model CTCM

The Corroded Tension Chord Model aims at predicting the load deformation behaviour of a crack element containing a reinforcing bar with a locally corroded section, induced e.g. by chloride ingress. It assumes that corrosion starts after cracking of the tension chord, i.e. that the cracking load was exceeded and the crack elements are defined. A damaged section of total length $\beta \cdot s_{rm}$ is assumed to be present at a crack (right end of crack element in Fig. 1 (right)), extending symmetrically into both adjoining crack elements. In this damaged section, the reinforcing bar has a reduced cross sectional area $A_{s,c} = (1-\zeta)A_s$ where ζ denotes the relative loss of cross section, i.e. $\zeta = A_{lost}/A_s$, $0 \le \zeta \le 1$, and bond is reduced to $\tau_{b,c} = \gamma\tau_b, 0 \le \gamma \le 1$, due to corrosion related bond degradation [8]. The concepts and equations of the TCM are extended, accounting for the behaviour in this damaged section.

Obviously, the length of the damaged section $\beta \cdot s_{rm}$ is a decisive parameter, which can strongly influence the residual deformation capacity. In a comprehensive study conducted by the Swiss Federal Roads Office [9], the corrosion parameters (number of corroded reinforcing bars, pit geometry, cross section loss, etc.) of 56 cantilever retaining walls were assessed. It revealed that typically, a single corrosion pit with a length in the order of 20 mm per reinforcing bar occurred. Thus, $\beta \cdot s_{rm} = 20$ mm (see Tab. 1) is adopted in this study. To investigate on the influence of bond deterioration, any model can be implemented (e.g. according to [8]) and the parameter γ can be determined accordingly. In this study, bond stresses in the damaged section are neglected, i.e. $\gamma = 0$, which is realistic except at low levels of corrosion.

Fig. 1 compares the stress distributions within a crack element containing a corroded reinforcing bar with a damage of $\zeta = 1 - f_y/f_u = 0.17$ (right, red line) to one containing an non-corroded reinforcing bar (left), loaded to the same stress at the crack of $\sigma_{sr} = 550$ MPa. For the numerical calculations, the material characteristics as listed in Tab. 1 and $\lambda = 0.5$ are considered.. To fulfil equilibrium, the reinforcing bar with undamaged cross section next to the damaged section exhibits a stress of $\sigma_s = \sigma_{sr}(1-\zeta) = 457$ MPa. The relatively moderate drop in stress of 17% represents the reduction in load-bearing capacity of the damaged crack element, and is equivalent to the reduction in cross-sectional area of the corroded reinforcing bar. When comparing the exhibited mean steel strains ε_{sm} (or the overall deformation), a reduction of 85% from the undamaged to the corroded element is observed, exemplarily showing the reduction in deformation capacity of the damaged element.

Table 1: Material characteristics and calculation parameters. Stress-strain relationship of used hot-rolled (HR) and cold-worked (CW) steel.

f_y	[MPa]	500	τ_{b0}	[MPa]	5.8
f_u	[MPa]	600	τ_{b1}	[MPa]	2.9
ε_{sh}	[-]	0.018	Ø	[mm]	20
ε_u	[-]	0.1	ρ	[-]	0.01
E_s	[GPa]	205	λ	[-]	1.0
f_c	[MPa]	30	s_{rm}	[mm]	495
f_{ct}	[MPa]	2.9	$\beta \cdot s_{rm}$	[mm]	20

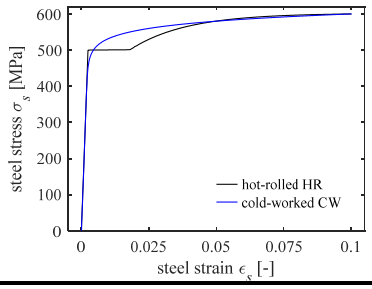

3 Effect of localised corrosion on load-deformation behaviour

3.1 Effect on a single crack element

Fig. 2 (left) shows the load-deformation behaviour of a single crack element of $s_{rm} = 495$ mm length containing a reinforcing bar with diameter 20 mm of hot-rolled steel, which is corroded to various degrees. Further material characteristics are given in Tab. 1. The response of a bare reinforcing bar is plotted for comparison (dashed line). Obvious is the much stiffer behaviour of the non-corroded crack

element (black line), compared to the response of the bare reinforcing bar, which is directly related to the tension stiffening effect.

The response of the crack element to the varying degrees of corrosion is shown with coloured lines, and a circle indicates the ultimate deformation at failure. Apparent is the disproportional reduction in deformation capacity with only slightly increasing corrosion, followed by a strong reduction in load-bearing capacity at higher degrees of corrosion.

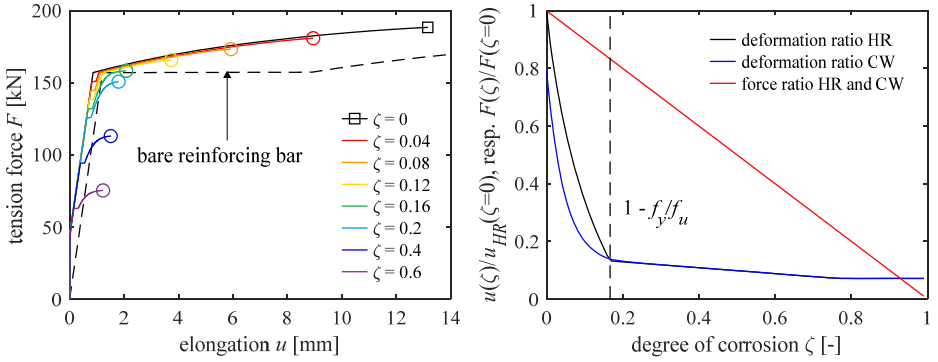

Fig 2: Load-deformation behaviour of a single crack element containing a hot-rolled reinforcing bar with various degrees of corrosion ζ (left). Circles indicate the failure of the crack element. On the right, maximum deformation of a crack element with a hot-rolled (HR) and a cold-worked (CW) reinforcing bar $u(\zeta)$, respectively, corroded to various extents, compared to a non-corroded crack element with hot-rolled steel $u_{HR}(\zeta=0)$. Additionally, as red line, the force ratio of a corroded to a non-corroded crack element is shown.

Fig. 2 (right) shows the ratio of deformation at failure for a crack element containing a hot-rolled (HR, black line) and a cold-worked (CW, blue line) reinforcing bar, respectively, with increasing degree of corrosion, compared to the deformation capacity of a crack element with a non-corroded HR reinforcing bar. Additionally, the ratio of load-bearing capacity of a crack element with corroded reinforcing bar compared to a crack element without any corrosion of the reinforcing bar is plotted. Similar to Fig. 2 (left), the strong decrease in deformation capacity for a comparably low corrosion damage is apparent: The deformation at failure is reduced by 85% at a relative loss of cross sectional area ζ of only 17%, whereas the failure load is reduced proportionally by 17%. For higher degrees of corrosion, the deformation capacity does not change significantly, whereas the load-bearing capacity further decreases proportionally with the cross section loss.

The strong reduction in deformation capacity in the beginning, up to a relative cross section loss of 17%, can be explained simply considering equilibrium: The failure load of the corroded part of the reinforcing bar is $F_{u,c} = A_{s,c} f_u = (1-\zeta) A_s f_u$. The yield load of the non-corroded part of the reinforcing bar is $F_y = A_s f_y$. Equating these forces and solving for ζ yields $\zeta = 1 - f_y / f_u = 17\%$. For a cross section loss smaller than 17%, the non-corroded part of the reinforcing bar is loaded above its yield point and experiences correspondingly large inelastic strains, whereas for a higher cross section loss, the remaining tensile resistance of the damaged section is not sufficient to yield the non-corroded part. The overall deformation therefore decreases strongly, as plastic strains only occur in the corroded part with a small length (in this example $\beta \cdot s_{rm} = 20$ mm). This effect is commonly known as strain localisation and was experimentally observed in several studies, e.g. [2,3]. Nevertheless, it has to be noted, that other phenomena like local bending moments and 3D stress states in the area of the pit can strongly influence the behaviour [2,10].

3.2 Assembling corroded and non-corroded crack elements

To analyse structural elements with several corroded and non-corroded reinforcing bars, crack elements are assembled serially and in parallel. The overall load-deformation behaviour of a tension chord consisting of several serially coupled crack elements can be modelled by summing up the deformations of the elements (at equal force). The number of corroded and non-corroded crack elements can be varied, applying the CTCM and the TCM to each element accordingly. Whereas this procedure assumes that

all crack elements are equally loaded, an increasing or decreasing tension chord force can be considered by discretising the force distribution, with the crack spacing specifying the discretisation length. Each element is then loaded differently, exhibiting a distinct deformation. Together with further structural mechanical concepts, this approach allows e.g. to predict the deflection of a cantilevering bridge deck with decreasing moment towards the parapet, with tension chords simulating the part around the upper reinforcement layer [11].

The load-deformation behaviour of several crack elements in parallel can be modelled by summing up their forces (at known elongation). Note that in contrast to serial crack elements, where the forces are equal by equilibrium, the elongations of parallel tension chords are not necessarily equal: As the corroded crack elements contain a weaker section, they exhibit bigger deformations at equal force than non-corroded crack elements. However, the assumption of equal deformations is often justified (similar to plane sections remaining plane), e.g. in cantilevers or retaining walls with a high in-plane stiffness. Hence, corroded and non-corroded crack elements, which exhibit equal elongations, can be assembled in parallel in good approximation by summing up their individually exhibited, distinct forces.

3.3 Effect on multiple crack elements

Fig. 3 (left) shows the load-deformation behaviour of 100 crack elements assembled in parallel, undergoing equal elongation, whereof 50 elements contain a corroded reinforcing bar. The cross section loss of the reinforcing bars varies within 4% and 60%. As dashed lines, the behaviour of 50 and 100 non-corroded crack elements is shown for comparison, and triangles indicate the peak load.

Similar to the observations in Fig. 2 (left) in Section 3.1, the deformation capacity of the entire structural element decreases up to a cross section loss $\zeta = 1 - f_y / f_u = 17\%$, followed by a strong reduction of the load-bearing capacity with further increasing corrosion damage. As soon as the corroded reinforcing bars rupture, the load drops to the capacity of the remaining 50 non-corroded crack elements, which still have their full strength and deformation capacity. However, one has to consider that in force-controlled situations, as it applies for the majority of the load cases, the structural elements fail when the maximum load is reached, i.e. the load and deformation indicated with a triangle. Hence, even moderate corrosion may cause a significant loss of deformation capacity.

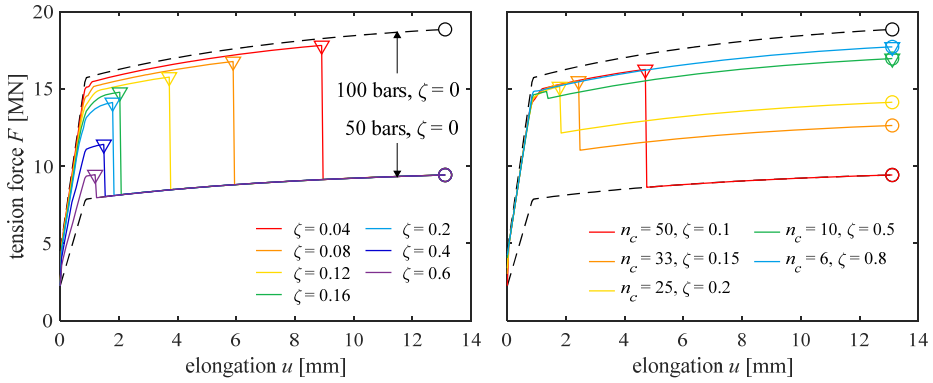

Fig. 3: Load-deformation behaviour of a structural element with 100 crack elements in parallel. $n_c = 50$ crack elements are corroded to an extent ζ (left); n_c crack elements are corroded to an extent ζ_i (right). The total cross section loss $\zeta_{tot} = \zeta_i \cdot n_c / 100$ is constant at 5%.

Fig. 3 (right) shows the load-deformation behaviour of a structural element consisting of 100 crack elements assembled in parallel, whereof n_c elements contain a corroded reinforcing bar with cross section loss of ζ_i. The total cross section loss $\zeta_{tot} = \zeta_i \cdot n_c / 100$ is kept constant at 5%. From the 94 possible pairs (n_c, ζ_i), a selection of 5 is depicted. As dashed lines, the behaviour of 50 and 100 non-corroded crack elements is shown for comparison, and triangles indicate the peak load.

Despite the constant total cross section loss ζ_{tot}, the load-bearing and deformation capacity decreases strongly for a decreasing number of corroded crack elements. This is due to the increasing cross section loss for each corroded crack element, in order to keep the total cross section loss constant. This

effect reverses from a specific number of corroded crack elements: For the pairs (n_c=10, ζ_i=50%) and (n_c=6, ζ_i=80%), the residual load-bearing capacity of the 90 and 94 non-corroded crack elements is higher than the load at failure of the corroded crack elements. This is noteworthy, as these structural elements therefore maintain their full deformation capacity at a just slightly reduced failure load.

In Fig. 4 (left), for the same structural element as before, the relative deformation capacity is plotted for all pairs (n_c, ζ_i) and for various total degrees of corrosion ζ_{tot}. Fig. 4 (right) shows the corresponding relative load-bearing capacity. Both figures indicate that it is generally less critical to have only a few reinforcing bars corroded to a high extent than vice versa, especially for a high total degree of corrosion $\zeta_{tot.}$ Furthermore, it is obvious that only indicating the total degree of corrosion is not sufficient to draw any conclusions on the load-deformation behaviour of a structure, as this depends on the corrosion distribution among the reinforcing bars of all crack elements.

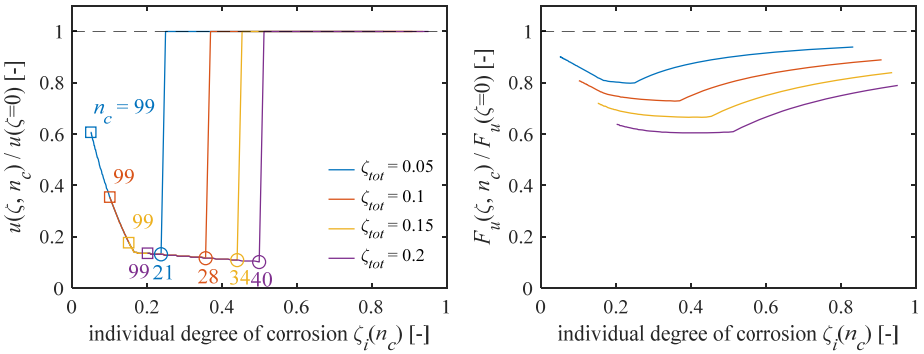

Fig. 4: Structural element assembled of 100 crack elements in parallel with a total degree of corrosion ζ_{tot}, containing n_c reinforcing bars with a cross section loss $\zeta_i = 100 \cdot \zeta_{tot} / n_c$. Relative load-deformation capacity (left); relative load-bearing capacity (right).

4 Ongoing experimental campaign for validation

As detected by a study of the Swiss Federal Roads Office [9], many existing retaining walls built in the 1960s and 1970s suffer from a severe local damage of the main tensile reinforcement at the construction joint above the footing, induced by atmospheric corrosion due to honeycombs. In this context, a large-scale experimental campaign was recently carried out in the Structures Laboratory of the Institute of Structural Engineering to explore the load-deformation behaviour of cantilevering retaining walls affected by localised pitting corrosion. A total of 8 wall segments of 2.0x1.7 m and 0.38 m thickness on a foundation of 2.1x1.4x0.4 m was tested in the Large Universal Shell Element Tester *LUSET* [12] (Fig. 5 (left)). The main tensile reinforcement consisted of 10 reinforcing bars of diameter 18 mm.

In a first series of 5 experiments, some of the bars of the main tensile reinforcement were mechanically damaged to various extents, using a spherical mill of diameter 20 mm. This type of „artificial corrosion“ was used for practicality to simulate increasing corrosion under applied load, since a preliminary investigation on bare bars had not revealed any relevant differences in the stress-strain behaviour compared to naturally corroded reinforcing bars. In the experiments, the wall base (foundation) was clamped. A combination of in-plane compression force, out-of-plane shear force, and bending moment was introduced at the top of the wall and increased until failure. Displacements were measured with a 3D Digitial Image Correlation System (DIC) and reinforcing bars were instrumented with a fibre optical strain measuring device [13]. In a second series of 3 experiments, after loading the specimens to service loads, 4 of 10 reinforcing bars were damaged stepwise during the experiment, simulating the increasing corrosion damage, by means of fully automatic drilling machines, which carried 20 mm spherical mills. Load was either kept constant or was decreased according the out-of-plane deflection of the wall head (hybrid-experiments), simulating the decreasing earth pressure action. To the authors' knowledge, these have been the first large-scale experiments with accelerated corrosion under constant or varying loads reported so far.

Fig. 5 (right) illustrates the preliminary results of the first 5 experiments with specifications given in Tab. 2 by plotting the measured bending moment at the wall footing versus the deflection of the wall head. Specimen RTW A, as reference test without any corrosion, exhibited the largest deformation at

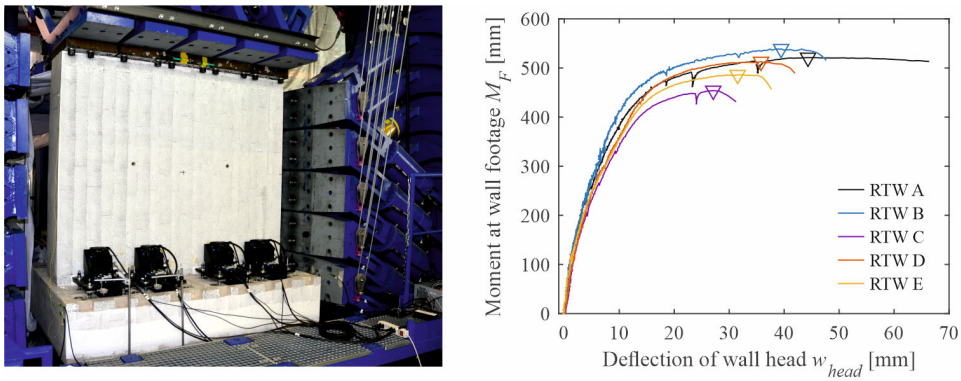

Fig. 5: Retaining wall segment in testing machine with installed drilling machines (left); bending moment at wall footing versus wall head deflection (preliminary results, right).

value depending on the corrosion damage. Specimen RTW B, with a total degree of corrosion ζ_{tot} = 3%, exhibited a reduction of 13% in deformation capacity. Specimens RTW C-E, with a total degree of corrosion ζ_{tot} = 9%, but corrosion assigned differently to each reinforcing bar (see Tab. 2), showed a reduction in deformation at peak load between 29% and 42%. Depending on the corrosion damage, the load-bearing capacity was reduced accordingly.

Very scarcely treated by the research community so far are additional effects related to localised corrosion pits, such as (i) the influence of the strain rate on the strength of reinforcing bars [14], (ii) different microstructures over the cross section for quenched and self-tempered reinforcing bars [15,16], (iii) the presence of a three-dimensional stress state in the vicinity of the pit [10] and (iv) local bending moments in unilaterally damaged reinforcing bars due to a shift in the neutral axis [10]. These effects may have a significant influence on the behaviour of corroded reinforced concrete structures, and the last two effects may e.g. explain the higher peak load of Specimen RTW B with slightly damaged reinforcing bars compared to Reference Test RTW A.

Table 2: Most relevant specifications on corrosion for specimens RTW A-E.

Specimen	# non-corr. bars	# corr. bars	deg. of corr. ζ_i per bar	tot. deg. of corr. ζ_{tot}
RTW A	10	0	-	0
RTW B	7	3	0.1	0.03
RTW C	7	3	0.3	0.09
RTW D	4	6	0.15	0.09
RTW E	5	5	[0.1, 0.15, 0.15, 0.2, 0.3]	0.09

5 Conclusions and Outlook

This paper introduced the Corroded Tension Chord Model CTCM, an expansion of the established Tension Chord Model TCM [4], which allows to calculate the load-deformation behaviour of concrete tension chords containing reinforcing bars affected by localised pitting corrosion on a sound mechanical basis. By assembling corroded and non-corroded crack elements in parallel and serially, it enables modelling entire structural elements, such as e.g. cantilevering retaining walls or bridge decks [11].

The calculations indicate a strong reduction of the deformation capacity of structures affected by local corrosion already at low or moderate cross section losses: The evaluated structures lost as much as 85% of their deformation capacity at an overall cross section loss of merely 17% (corresponding to the point beyond which the tensile strength of the damaged section is no longer capable of generating inelastic deformations in the remaining parts of the tension chord). This reduction is disproportionate to the decrease in load-carrying capacity, which is proportional to the cross section loss. Calculations further reveal the complexity of the issue when structures are analysed, which contain several parallel tension chords with different numbers of corroded reinforcing bars and varying corrosion degree, but exhibit an equal total corrosion damage. Structures with few heavily corroded reinforcing bars seem to

be less critical regarding load-bearing and deformation capacity than structures with a large number of slightly corroded reinforcing bars. However, specific information on the distribution of corrosion among the reinforcing bars is mostly missing in practice for existing structures, causing considerable uncertainty regarding the accurate assessment of the structural safety. Further complexity arises because of the probabilistic nature of initiation and spreading of local corrosion in the region of the governing section. Additionally, a change in the load-transfer mechanism due to the change in stiffness (e.g. in slabs subjected to concentrated loads) has not yet been analysed.

Localised corrosion of reinforcing bars causes further effects, such as e.g. a 3D stress state or local bending moments at the corrosion pits [10], which have only scarcely been treated in literature in this context. These effects may have a major influence on the load-deformation behaviour of corroded concrete structures and corresponding mechanical models are partly missing. The authors are currently investigating on these topics in order to include them in the CTCM.

References

[1] Cairns, J., Plizzari, G. A., Du, Yingang, L., David W., and Ch. Franzoni. 2005. "Mechanical Properties of Corrosion-Damaged Reinforcement." *ACI Materials Journal* 102: 256-64.

[2] Andisheh, K., Scott, A., and A. Palermo. 2016. "Modeling the influence of pitting corrosion on the mechanical properties of steel reinforcement." *Materials and Corrosion* 67:1220-34. doi:10.1002/maco.201508795.

[3] Chen, E., Berrocal, C. G., Fernandez, I., Löfgren, I., and K. Lundgren. 2020. "Assessment of the mechanical behaviour of reinforcement bars with localised pitting corrosion by Digital Image Correlation." *Engineering Structures* 219. doi: 10.1016/j.engstruct.2020.110936.

[4] Marti, P., Alvarez, M., Kaufmann, W., and V. Sigrist. 1998. "Tension Chord Model for Structural Concrete." *Structural Engineering International* 8:287-98. doi:10.2749/101686698780488875.

[5] Lim, S., Mitsuyoshi, A., and D. M. Frangopol. 2016. "Assessment of the structural performance of corrosion-affected RC members based on experimental study and probabilistic modelling." *Engineering Structures* 127:189-205. doi:10.1016/j.engstruct.2016.08.040.

[6] Azad, A. K., Ahmad, S., and S. A. Azher. 2007. "Residual Strength of Corrosion-Damaged Reinforced Concrete Beams." *ACI Materials Journal* 104-M05:40-47.

[7] Kaufmann, W., and P. Marti. 1998. "Structural Concrete: Cracked Membrane Model." *Journal of Structural Engineering* 124:1467-75. doi:10.1061/(ASCE)0733-9445(1998)124:12(1467).

[8] fib Bulletin 10. 2000. *Bond of reinforcement in concrete.* Lausanne: fib fédération internationale du béton.

[9] Swiss Federal Roads Office FEDRO. 2014. *Evaluation de l'état des mures de soutènement béton à semelle. Etude pilote. Rapport de synthèse des phases 1 et 2.* Swiss Confederation, Bern.

[10] Hingorani, R., Pérez, F., Sánchez, J., Fullea, J., Andrade, C., and P. Tanner. 2013. "Loss of ductility and strength of reinforcing steel due to pitting corrosion." Paper presented at the VIII Int. Conf. on Fracture Mechanics of Concrete and Concrete Structures, Toledo, March 10-14.

[11] Yilmaz, D., Haefliger, S., Kaufmann, W., and U. Angst. 2020. "New conceptual approach combining the probabilistic nature of localised rebar corrosion and the load-deformation behaviour." Paper presented at the 2nd CACRCS Workshop 2020 Online, December 1-4.

[12] Kaufmann, W., Beck, A., Karagiannis, D., and D. Werne. 2019. *The Large Universal Shell Element Tester LUSET.* Zürich: ETH Zürich, Institute of Structural Engineering.

[13] Mata-Falcon, J., Haefliger, S., Lee, M., Galkovski, T., and N. Gehri. 2020. "Combined application of distributed fibre optical and digital image correlation measurements to structural concrete experiments." *Engineering Structures* 225. doi:10.1016/j.engstruct.2020.111309.

[14] Haefliger, S., Fomasi, S., and W. Kaufmann. 2020. "Influence of strain rate on the stress-strain characteristics of modern reinforcing bars." *Construction and Building Materials.* Submitted for Publication.

[15] Hortigón Fuentes, B., Gallardo Fuentes, J. M., Muñoz Moreno, S., Gümpel, P., and J. Strittmatter. 2018. "Wirkung der Tempcore-Behandlung auf die Zugeigenschaften von Stabstahl." *Stahl und Eisen* 138:45-52.

[16] Haefliger, S., and W. Kaufmann. 2020. "Influence of corrosion on the stress-strain characteristics of quenched and self-tempered reinforcing bars." *Construction and Building Materials.* Submitted for Publication.